EVOLUTIONARY BIOLOGY

A universal scaling law of mammalian touch

J. W. Andrews[1], M. J. Adams[2], T. D. Montenegro-Johnson[1]*

For most mammals, touch is the first sense to develop. They must feel vibrations on the surface of their skin to enable them to respond to various stimuli in their environment, a process called vibrotaction. But how do mammals perceive these vibrations? Through mathematical modeling of the skin and touch receptors, we show that vibrotaction is dominated by "surface" Rayleigh waves traveling cooperatively through all layers of the skin and bone. Applying our model to experimental data, we identify a universal scaling law for the depth of touch receptors across multiple species, indicating an evolutionarily conserved constant in the sensation of vibrations.

INTRODUCTION

When a person slides a finger across a surface, or when elephants communicate long distances with their feet (*1*–*5*), vibrations travel through the skin, exciting mechanoreceptors; these are nerve endings that convert mechanical vibrations to electrical signals. Subsequently, the recruited mechanoreceptors transmit the signal to the brain, which interprets it as a tactile experience. For a human, this vibrotactile signal allows differentiation between textures, manipulation of objects, and detection of initial contact, while for the elephant, the signal might indicate a mate or the presence of vehicles. Humans, elephants, and other mammals all rely on extracting fine detail from vibrational feedback.

Touch is a primordial sense. Our common ancestor with elephants (and other mammals), the 160-million-year-old Chinese Juramaia (*6*), certainly had and relied on touch. However, the properties of mammalian skin vary wildly between different species; the hide of an elephant is about 400 times stiffer, and a factor of 16 thicker, than that of a human. Even among humans, skin stiffness varies with age, gender, location on the body, and even profession by an order of magnitude. Skin stiffness can even change in a single individual based on their hydration level (*7*). How, then, do mammals perceive vibrations? What waves travel through their bodies to allow constancy of perception, when the properties of the skin can be so different?

All mammalian skin is a layered, inhomogeneous viscoelastic solid comprising the outermost epidermis, followed by the dermis and then hypodermis, which have similar mechanical properties. A schematic diagram of our model skin structure is shown in Fig. 1. The outer sublayer of the epidermis, the stratum corneum, is much stiffer than the other layers; this is important since it is the stratum corneum that makes direct contact with oscillating sources that generate the waves that travel through the skin.

Touch is a remarkably complicated sense, using several different types of mechanoreceptors to detect skin waves. The mechanoreceptors are located within the skin layers and comprise four types—viz., the Merkel's disk, Meissner's corpuscles, Ruffini endings, and Pacinian corpuscles (PCs)—although the nomenclature varies across species. We will focus on the PCs, which are the mechanoreceptors that enable the perception of mechanical vibrations ranging between 20 and 1000 Hz, with approximately 100 to 1000 Hz being the most relevant to touch (*7*). The PCs lie deep within the skin near the dermis/hypodermis boundary (*7*). They are not fully free to move but rather held in place by a network of facia, which magnifies the forces they experience from incident waves (*8*). Furthermore, the PCs are capable of detecting submicron features (*9*), enable nonlocal detection (>10 cm) far from the initial site of excitation, and are phasic, i.e., they rapidly reduce their electrical response following an initial mechanical stimulus (*10*).

It is generally accepted (*11*) that PCs respond to P- (compression) waves (*12*), based primarily on modeling. In such studies, only S- (shear) waves and P-waves were considered. However, it has become increasingly evident that Rayleigh (surface-traveling) waves may also play an important role (*13*). Moreover, it has yet to be resolved whether nonlocal waves are transmitted either along the skin (*14*) or through the bone (*2*). The physics of these wave types are described in section S5.

Upon noting the complexity of traveling waves through the skin, their penetration, dispersion, and reflections (*15*), Nobel laureate G. von Békésy commented "I have always hoped that geologists in the study of earthquake waves would throw light on the nature of Rayleigh waves and Lamb waves." Here, we develop the "elaborate formulation" that von Békésy requested: a mathematical model for the propagation of elastic waves through a layered elastic structure (Fig. 1) with a range of properties that are similar to mammalian skin.

Our formulation demonstrates that viscoelasticity contributes only to wave damping in the case of vibrotaction. Consideration is given to the propagation of three permissible wave types—P-, S-, and Rayleigh waves—each with radically different properties. Coupling this analysis to a mathematical model of the PCs, we show that vibrotaction is governed by long-wavelength Rayleigh waves. Although "surface" waves, they, in fact, travel cooperatively through all skin layers and the bone (not either-or, as previously argued). Applying our model to experimental data across multiple mammalian species, we show that the depth of the PCs (DPC) is evolutionarily conserved to respond to Rayleigh rather than P-waves (*16*–*25*).

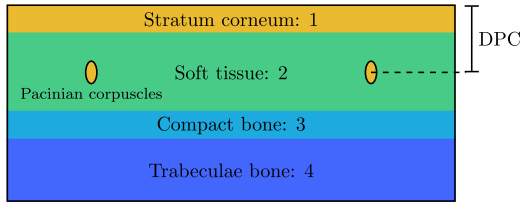

Fig. 1. Schematic of our skin model (layer thicknesses not to scale), showing the DPC. Layers are numbered as in the governing equations.

[1]School of Mathematics, University of Birmingham, Edgbaston, Birmingham B15 2TT, UK. [2]School of Engineering, University of Birmingham, Edgbaston, Birmingham B15 2TT, UK.
*Corresponding author. Email: t.d.johnson@bham.ac.uk

RESULTS

The mathematics underlying the physics of touch is remarkably similar to that of earthquakes. In 1898, Bromwich (*26*) developed an approach to determine the wave properties of a thin elastic layer over a semi-infinite elastic layer. He concluded that the work was not appropriate for earthquake modeling and was generally ridiculed in later works by other authors, especially by Love in 1911 (*27*). In 1914, Lamb extended the approach of Bromwich (*26*) for the waves generated on elastic layers of increasing thickness. The increasing depth of each layer has had a substantial impact on sensor design and radar evasion throughout the 20th century. The approach developed by Lamb (*28*) is amenable to the analysis of a series of elastic layers and can be extended to viscoelastic layers if required (*29*), which forms the basis of our analysis (see section S4).

For pure elastic theory to be applicable, the propagating waves must not be viscoelastic in nature, and the viscous decay should be sufficiently small per wavelength. The conditions for a viscoelastic wave to exist in our model are not satisfied (section S2), and hence, all waves are fundamentally elastic waves, modified by the inclusion of an exponentially decaying amplitude with a number of wavelengths. The viscous contribution to the decaying amplitude is $e^{-\gamma\lambda t}$, where γ is a measure of the viscosity of the layer, t is the time of travel for the wave, and λ is the wavelength. Experimental values for γ are small (0.226 s^{-1} m^{-1}) (section S2) (*30*), and thus, viscoelasticity does not become significant except for long times or large distances. The relevant distance is approximately 1 to 2 m for humans (a more detailed analysis may be found in section S2. Consequently, we proceed with the modified elastic theory.

Earthquakes generate P- (*27*), S- (*27*), Rayleigh (*27*), and Love waves (*27*). P- and S-waves travel through the bulk, whereas Rayleigh and Love waves propagate along surfaces. From an energy perspective, surface waves spread over a smaller number of dimensions, and thus, the amplitudes decay more slowly than the body (P- and S-) waves. Rayleigh waves typically deliver the most energy in an earthquake, since their disturbance remains high for greater distances than P- or S-waves. It should be emphasized, however, that near to the epicenter, P- and S-waves can dominate the energy.

The amplitude of Rayleigh waves decays rapidly with the depth of the elastic medium (*28*). Consequently, Rayleigh waves are typically ignored at any depth exceeding their wavelength. Earthquakes typically involve interactions where the elastic layers are thick compared to the wavelength of the propagating waves (*27*). However, touch entails elastic layers that are thin compared to these wavelengths; the implications have not been considered previously, which is addressed in the current work.

Absence of Love waves

Love waves are surface waves that can exist in layered materials. Since the mechanoreceptors are located very near the boundary between layers, it might be expected that they would be ideal waves to excite a variety of mechanoreceptors. The surface wave property means that they travel efficiently through a layer with little loss of energy, allowing the wave to propagate for extended distances. However, Love waves are also capable of creating Rayleigh waves, adding noise to the original signal, which would not be a desirable effect for tactile sensation.

For Love waves to exist, there are a range of conditions that need to be satisfied. The first, most famous condition, is that a Love wave exists in the layer with the fastest S-wave when compared with adjacent layers. The layers where the S-wave condition is satisfied do not correspond to the layers where the mechanoreceptors are located. This alone suggests that Love waves are not responsible for touch. In addition, the second condition for Love waves to exist requires that the layer is sufficiently thick to support the wave and corresponds to a thickness of 0.8λ (*27*). This minimum thickness condition is not satisfied for any of the layers in any of the mammal species considered (table S2). Consequently, Love waves are not considered further as a possible means of exciting mechanoreceptors in mammals.

Rayleigh waves in skin

For simplicity, we number the skin layers from 1 to 4, with the numbers increasing into the depth of the skin and bone (1 is stratum corneum, 2 is soft tissue, etc.), as in Fig. 1. We will begin by calculating the dispersion relation for Rayleigh waves in our skin model. The dispersion relation connects the frequency of a wave to its speed. However, it also describes the properties of the wave except for its original amplitude at generation. Hence, most of the important physics for our system can be obtained from a dispersion relation: for instance, the phase velocity and the spreading of a group of frequencies, which are key when locating and analyzing a signal. Furthermore, a solution to the dispersion relation ensures that cooperative Rayleigh waves exist in this system.

The dispersion relation for Rayleigh waves traveling through our model layered structure—asymptotically expanded since layer thickness/wavelength, (h_i/λ), is small—is given at leading order by (see section S5 for details of the derivation and accompanying fig. S4)

$$(2-\xi^2)^4 - 16(1-\alpha^2\xi^2)(1-\xi^2) = \underbrace{\beta\left[-0.522\frac{2\pi\rho_0 h_0}{\lambda\rho_4}\right]}_{\text{Liquid layer}} + \underbrace{\frac{4}{\lambda}\xi^2(1-\xi^2)\sum_{i=1}^{3}\left\{h_i\left(1-\frac{A_{i+1}}{A_i}\right)\left[\frac{\rho_i}{\rho_4}-\frac{\mu_i}{\mu_4}\right]\right\}}_{\text{Elastic layers}} \quad (1)$$

where ξ is the ratio of the Rayleigh wave speed to the S-wave in the trabeculae bone; α is a ratio of the Poisson's ratio as defined in the Supplementary Materials (section S5); λ is the wavelength of the Rayleigh wave; h_i is the thickness of the i-th layer; ρ_i is the density of the i-th layer; and $A_i = \sqrt{1-c^2/c_i^2}$, with c_i the speed of the S-wave in the i-th layer, and c the speed of the Rayleigh wave. The term β takes the value 1 if the mammal is aquatic and 0 otherwise. Last, μ_i is the second Lamé constant for each of the elastic layers. The dispersion relations for P- and S-waves are given in the Supplementary Materials (eqs. S4 and S5; parameters for layers are shown in table S1).

Having derived the dispersion relation, we require two more pieces of information to understand skin waves and that Rayleigh waves dominate vibrotaction. The first is how waves are generated in an elastic structure by an oscillating excitor, and the second is how the PCs respond to these incoming waves.

The result in Fig. 2 shows that P- and S-waves decay more quickly away from the site of excitation when compared to Rayleigh waves (section S6), as expected from a conservation of energy argument applied to the amplitude. For P- and S-waves, this decay in the layered structure is calculated in the standard manner (*27*). For Rayleigh waves, the solution of Lamb has been modified and the material properties of the skin depth averaged. The averaging process involves solving the dispersion relation (Eq. 1) to obtain wave properties and

then determining which averaged material properties are required to yield the same wave behavior when solving the dispersion relation given by Lamb (*28*).

The generation of waves due to oscillations depends on the exact nature of the contact. However, the amplitudes of the three potential waves in decreasing strength are P-waves, Rayleigh waves, and S-waves. P-waves radiate S-waves at all interfaces, and so, they dissipate energy to S-waves as they propagate. S-waves generate Rayleigh waves of low amplitude at each interface between the layers. These secondary Rayleigh waves are unlikely to be detected because of their small amplitude, so confusion due to this source is unlikely.

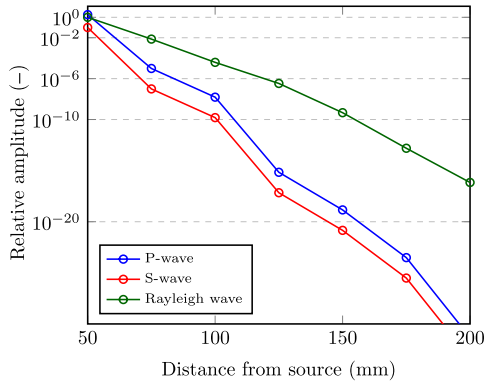

Fig. 2. Decay of skin waves. The amplitude (relative to P-wave amplitude at 5 cm) of all three permissible wave types as a function of distance from a sphere of radius 8 mm oscillating normal to the skin at a frequency of 200 Hz, showing a relatively slow decay of the Rayleigh wave (section S6).

PCs filter P-waves

To complete our study, we further required a model of the PCs to establish how the mechanoreceptor might be excited by different incoming waves. A schematic of the model is shown in Fig. 3A, with further details in section S1. The structure of the PC comprises a stiff outer layer, encapsulating a series of lamella. These lamellae form an onion-like structure, with a viscous fluid (assumed to be water) between them. The number of layers in the onion varies but is typically in the range of 30 to 60. Full mathematical details are available in (*7*). As has been demonstrated in previous studies [for a summary, see (*16*)], S-waves are significantly reduced by the structure of the PCs and so are not likely to elicit a response in the nerve at the core. While P-waves have the most energy of any of the waves, most of this energy corresponds to the zeroth mode (see Fig. 3B). Figure 3C shows that the structure of the PC filters out the zeroth mode of deformation (pure radial oscillation) almost entirely, as reasoned (but not shown mathematically) in previous studies (*16*). Thus,

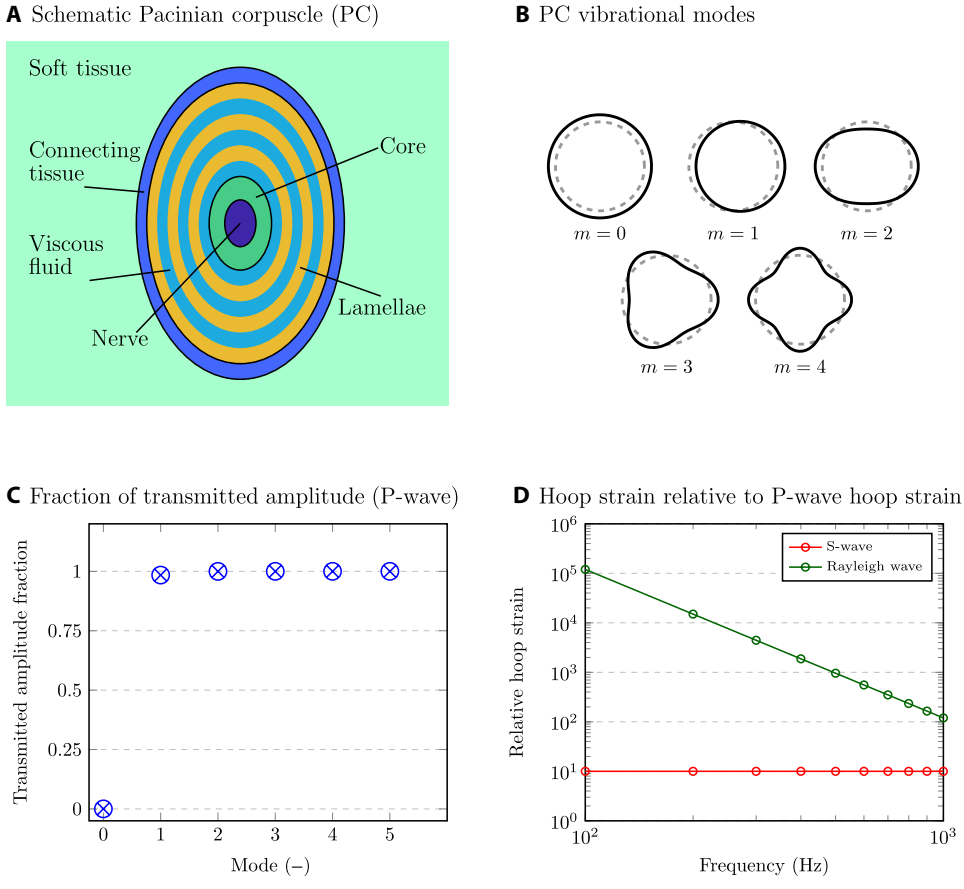

Fig. 3. Wave interaction with the PCs. (**A**) Schematic of our model of the PCs (full details in the Supplementary Materials). (**B**) Example of excitation modes for a PC. (**C**) Filtering of the P-wave excitation modes by the structure of the PC, showing that the dominant mode 0 is filtered out. (**D**) Rayleigh and S-wave amplitudes transmitted to the core of the Pacinian, relative to P-waves, for a range of frequencies, showing the dominance of the Rayleigh wave signal.

most of the P-wave energy is not transmitted to the nerve in the center of the PC, and Fig. 3D demonstrates that Rayleigh waves preferentially excite the PCs. The Rayleigh wave elicits about 100 to 10,000 times the effect of a P-wave, depending on frequency. As in Fig. 2, a Rayleigh wave decays more slowly than the other waves and so persist for longer, allowing for long-range and temporal discrimination of signals. These two results demonstrate that the dominant exciter of the PCs is the Rayleigh waves.

Rayleigh waves travel cooperatively through all material layers

The amplitude decay of Rayleigh waves into the tissue is less than 2.5% for typical detection frequencies of the PCs at the surface of the bone. This is a direct consequence of the wavelength being significantly longer than the depth of the soft tissue. Physically, this wave is indeed a Rayleigh wave, i.e., it moves the material in a retrograde motion. In our case, a wave satisfying the dispersion relation is able to exactly match the retrograde motion with the next layer and allow the wave to penetrate to the next layer and so on until the bone is reached. Furthermore, not only are the displacements matched between layers, but also the appropriate stress conditions are matched.

For humans, a 1-μm oscillating contact will produce a vibration with an amplitude of 0.975 μm; this demonstrates that the decay for the cooperative Rayleigh wave is not significantly attenuated at the bone from the surface. As a result, these long-range skin waves travel neither across the surface nor through the bone but through all layers of the skin and bone simultaneously.

Perceptual constancy in humans

With our model, we are also able to examine the effects of changing the stiffness of the outermost layer of skin, the stratum corneum, on the propagated waves. This is important, since people of different ages/genders/careers have a wide range of skin stiffnesses yet are all able to reliably differentiate textures via vibrotaction. Even hydration levels in an individual can change the stiffness of the stratum corneum by orders of magnitude. Figure 4 demonstrates that while P- and S-waves are significantly affected by the stiffness of stratum corneum (a proxy for hydration levels), the Rayleigh wave is almost completely insensitive over the entire range of values. Equally, for such variation in stiffness, there is little effect on the amplitude of a Rayleigh wave that is initiated by a controlled surface deformation excitation. This is because the effective "averaged" stiffness of the tissue is largely unaffected by changes in the thin stratum corneum when considering Rayleigh waves (see section S5). This provides further support to our argument that Rayleigh waves dominate vibrotaction.

The interaction of Rayleigh waves with PCs is evolutionarily conserved across large mammals—A universal scaling law

Rayleigh waves are relatively insensitive to the mechanical properties of skin, provided that the wavelength relative to the DPC is >1. For a range of different mammals, these values are given in table S1. Plotting the ratio of the wavelength of the Rayleigh wave to the DPC in Fig. 5 demonstrates that most species lie on a straight line with a gradient of approximately 5/2, i.e., the ratio of the skin Rayleigh wavelength to the depth of the mechanoreceptors is approximately constant across mammalian species.

Since the value of this evolutionarily conserved constant is >1.25 in the species considered, it is unlikely that any mammal will have sufficiently thick skin to permit Love waves (sections S3 and S7). The complicated interactions of Love waves and Rayleigh waves are thus avoided. Furthermore, none of the mammals correspond to a parametric space that will permit hydration levels to greatly affect the response of the PCs. Therefore, Rayleigh waves are the basis of perceptual constancy for all the mammalian species considered. Furthermore, all mammals lying on the line with a gradient of 5/2 will have the same sensitivity to a given skin displacement, although a greater force is required for this displacement, for example, on a sperm whale compared with a human. This means that any mammal on the 5/2 line might be expected to respond in the same manner to a stimulus that causes the same skin displacement. The rodents in Fig. 5 lie significantly above the 5/2 line, apparently making them more sensitive to skin surface displacements than other mammals. There are several possible explanations for the discrepancy.

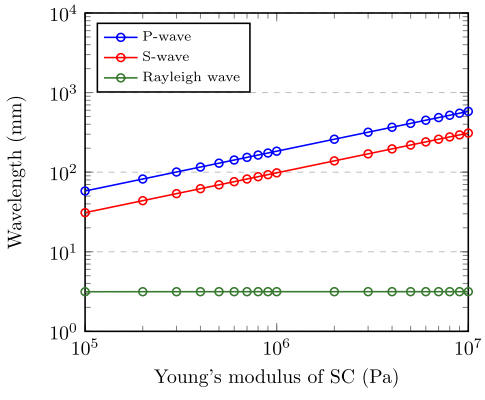

Fig. 4. Properties of skin Rayleigh waves are insensitive to hydration levels. As the stiffness of the stratum corneum (SC), a proxy for hydration levels, varies, the wavelength of the P- and S-waves changes considerably, while the Rayleigh wave remains largely unaffected. Range of Young's moduli was taken from experimental data (*2*). Location of the body is the forearm data and a frequency of 200 Hz.

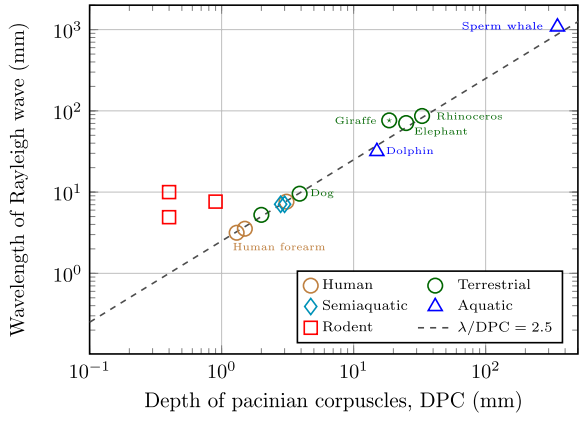

Fig. 5. Across a range of mammals of varying sizes, including aquatic and semiaquatic species, but excluding rodents, the ratio of the skin Rayleigh wavelength to the DPC is evolutionarily conserved, with an approximate value of 5/2. Note that the hypervasculated skin of the giraffe is not incorporated in our model, and hence, the giraffe lies slightly off the trend line. Source of data (*32*–*43*).

First, note that the reported Young's modulus of rodent skin is similar to humans and not softer as would be required for the 5/2 law. Perhaps there is a minimum Young's modulus of skin required to maintain skin integrity?

Second, the PCs are of comparable size relative to the limbs of rodents, and the number they can contain is thus limited. The location of the PCs are thus different for rodents, being found along the tendons, whereas nonrodents tend to have their PCs located at either side of the tendons. This difference is caused by the size of the mammal; geometrically, there are fewer options regarding the possible positions of PCs. The wave transmission properties of tendons, which depend on the tension of the tendon, may thus be exploited in rodents, as may excitation via standing waves (section S8). It is known that the location of PCs in developing humans in utero is similar to that of the rodents (*31*).

Third, perhaps rodents simply benefit from being more sensitive to vibrations than their predators or can use the excited tendons to receive enhanced directional information? Last, the rodents investigated were laboratory specimens that will have undergone different selective pressures than might be expected in the wild. Moreover, it is also important to note that rodents tend to have a lower proportion of bone compared with the other mammals considered in table S1, and since this model does not take this into account, the discrepancy could be due to the greater proportions of cartilage.

DISCUSSION

We have developed a mathematical model of the process of vibrotaction, comprising a layered viscoelastic solid coupled to a model of the PC mechanoreceptors, in response to von Békésy's call for an elaborate formulation based on the mathematics of earthquakes to examine the properties of Rayleigh and Love waves in the skin. While von Békésy drew analogies between touch and wave propagation in the cochlea, our model shows the analogy holds that the PCs are most excited by surface Rayleigh waves and that these Rayleigh waves travel, not along the surface per se, but cooperatively through all layers of bone and skin (not either-or, as often posited). We furthermore showed that the properties of the Rayleigh waves (unlike the P- and S-waves) in the skin are not significantly affected by hydration levels (which can affect the stiffness of the outermost layer of skin by several orders of magnitude), allowing for perceptual constancy in individuals. Last, we found that there exists a universal scaling law across mammals (except small rodents) for all species with available data, viz., the ratio of the wavelength of a Rayleigh wave in the skin to the depth of mechanoreceptors is approximately equal to 5/2.

We note that since the model developed here represents a bone-supported structure, it should only be applied to sections of mammalian bodies exhibiting this feature. Typically, our model may be expected to apply to limbs, the head, and neck, but the thorax, for example, is not usually supported in a similar manner for most mammals. Thus, the model should be modified accordingly before being applied to such regions. However, it should be emphasized that most mammals have the PCs in the thorax at far more scattered locations compared with the regular depths found elsewhere in the body. The model may, however, be used for both glabrous and hairy skin.

Last, we note that other animals, notably birds and lizards, have mechanoreceptors that have similar structures to PCs. As a result, we might reasonably expect this conserved quantity to be preserved across other classes of animal, although currently, the requisite experimental data are not available.

MATERIALS AND METHODS

The objective of this study is to determine the amount that different wave types in skin contribute to the sensation of vibrations, i.e., vibrotaction. Mathematical analysis of the Cauchy momentum equations of motion for elastic solids was performed for layered materials (see the Supplementary Materials) with viscous decay, and the permissible wave types were analyzed. An asymptotic reduction of the governing equations for Rayleigh waves was used to calculate the dispersion relation (Eq. 1).

An investigation of the relative amplitudes required for the three permissible waves—P-, S-, and Rayleigh waves—and how these waves decay away from the source of excitation was performed. The interaction between these waves and the PCs was modeled as described by Bell *et al.* (*7*) and as elaborated in the Supplementary Materials. Evaluation of the relevant equations for various input parameters was performed in MATLAB.

Parameters were taken from literature, provided by Wiertlewski and Hayward (*31*), while the variation in the elastic properties of the stratum corneum is found in the work of Sednaoui *et al.* (*3*). All parameters are supplied in section S2.

SUPPLEMENTARY MATERIALS

Supplementary material for this article is available at http://advances.sciencemag.org/cgi/content/full/6/41/eabb6912/DC1

View/request a protocol for this paper from *Bio-protocol*.

REFERENCES AND NOTES

1. M. Wiertlewski, C. Hudin, V. Hayward, On the 1/f noise and non-integer harmonic decay of the interaction of a finger sliding on flat and sinusoidal surfaces, in *2011 IEEE World Haptics Conference*, Istanbul, Turkey, 21 to 24 June 2011, pp. 25–30.
2. M. J. Adams, S. A. Johnson, P. Lefèvre, V. Lévesque, V. Hayward, T. André, J. L. Thonnard, Finger pad friction and its role in grip and touch. *J. R. Soc. Interface* **10**, 20120467 (2013).
3. T. Sednaoui, E. Vezzoli, B. Dzidek, B. Lemaire-Semail, C. Chappaz, M. Adams, Friction reduction through ultrasonic vibration part 2: Experimental evaluation of intermittent contact and squeeze film levitation. *IEEE Trans. Haptics* **10**, 208–216 (2017).
4. C. E. O'Connell-Rodwell, Keeping an "ear" to the ground: Seismic communication in elephants. *Physiology* **22**, 287–294 (2007).
5. D. M. Bouley, C. N. Alarcon, T. Hildebrandt, C. E. O'Connell-Rodwell, The distribution, density and three dimensional histomorphology of Pacinian corpuscles in the foot of the Asian elephant (*Elephas maximus*) and their potential role in seismic communication. *J. Anat.* **211**, 428–435 (2007).
6. H. Kuhn, L. Humeniuk, N. Kozlov, S. Roigas, S. Adel, D. Heydeck, The evolutionary hypothesis of reaction specificity of mammalian ALOX15 orthologs. *Prog. Lipid Res.* **72**, 55–74 (2018).
7. J. Bell, S. Bolanowski, M. H. Holmes, The structure and function of Pacinian corpuscles: A review. *Prog. Neurobiol.* **42**, 79–128 (1994).
8. T. Hasegawa, K. Yosioka, Acoustic-radiation force on a solid elastic sphere. *J. Acoust. Soc. Am.* **46**, 1139–1143 (1969).
9. T. Miyaoka, Submicron-texture-discrimination mechanisms in human tactile perception. *Proc. Fechner Day* **24**, 151–156 (2008).
10. M. Sato, Response of Pacinian corpuscles to sinusoidal vibration. *J. Physiol.* **159**, 391–409 (1961).
11. T. Nara, M. Takasaki, T. Maeda, T. Higuchi, S. Ando, S. Tachi, Surface acoustic wave tactile display. *IEEE Comput. Graph. Appl.* **21**, 56–63 (2001).
12. B. Delhaye, V. Hayward, P. Lefèvre, J. L. Thonnard, Texture-induced vibrations in the forearm during tactile exploration. *Front. Behav. Neurosci.* **6**, 37 (2012).
13. R. S. Johansson, U. Landström, R. Landström, Responses of mechanoreceptive afferent units in the glabrous skin of the human hand to sinusoidal skin displacements. *Brain Res.* **244**, 17–25 (1982).

14. S. Saha, R. S. Lakes, The effect of soft tissue on wave-propagation and vibration tests for determining the in vivo properties of bone. *J. Biomech.* **10**, 393–401 (1977).
15. G. von Békésy, *Sensory Inhibition* (Princeton Univ. Press, 2017).
16. N. Cauna, G. Mannan, Development and postnatal changes of digital Pacinian corpuscles (*corpuscula lamellosa*) in the human hand. *J. Anat.* **93**, 271–286 (1959).
17. R. S. Johansson, A. B. Vallbo, Tactile sensibility in the human hand: Relative and absolute densities of four types of mechanoreceptive units in glabrous skin. *J. Physiol.* **286**, 283–300 (1979).
18. D. Metze, T. Luger, Nervous system in the skin, in *The Biology of the Skin* (The Parthenon Publishing Group, New York, 2001) pp. 153–176.
19. V. K. Affolter, P. F. Moore, Histologie features of normal canine and feline skin. *Clin. Dermatol.* **12**, 491–497 (1994).
20. J. H. Plochocki, S. Ruiz, J. R. Rodriguez-Sosa, M. I. Hall, Histological study of white rhinoceros integument. *PLOS ONE* **12**, e0176327 (2017).
21. Y. Moayedi, L. F. Duenas-Bianchi, E. A. Lumpkin, Somatosensory innervation of the oral mucosa of adult and aging mice. *Sci. Rep.* **8**, 9975 (2018).
22. G. Patrizi, B. L. Munger, The cytology of encapsulated nerve endings in the rat penis. *J. Ultrastruct. Res.* **13**, 500–515 (1965).
23. J. T. Haldiman, W. G. Henk, R. W. Henry, T. F. Albert, Y. Z. Abdelbaki, D. W. Duffield, Epidermal and papillary dermal characteristics of the bowhead whale (Balaena mysticetus). *Anat. Rec.* **211**, 391–402 (1985).
24. M. A. Al-Aqaba, F. S. Anis, I. Mohammed, H. S. Dua, Nerve terminals at the human corneoscleral limbus. *Br. J. Ophthalmol.* **102**, 556–561 (2018).
25. V. P. Eroschenko, *DiFiore's Atlas of Histology with Functional Correlations* (Lippincott Williams & Wilkins, 2008).
26. T. I. Bromwich, On the influence of gravity on elastic waves, and, in particular on the vibrations of an elastic globe. *Proc. Lond. Math. Soc.* **s1-30**, 98–165 (1898).
27. A. H. Love, Chapter XI: Theory of the propagation of seismic waves, in *Some Problems of Geodynamics* (Cornell Univ. Library, 1911), pp. 144–178).
28. H. Lamb, On waves in an elastic plate. *Proc. R. Soc. Lond.* **93**, 114–128 (1917).
29. P. K. Currie, M. A. Hayes, P. M. O'Leary, Viscoelastic Rayleigh waves. *Q. Appl. Math.* **35**, 35–53 (1977).
30. H. Lamb, On the propagation of tremors over the surface of an elastic solid. *Proc. R. Soc. Lond.* **203**, 1–42 (1904).
31. M. Wiertlewski, V. Hayward, Mechanical behavior of the fingertip in the range of frequencies and displacements relevant to touch. *J. Biomech.* **45**, 1869–1874 (2012).
32. J. Genzer, J. Groenewold, Soft matter with hard skin: From skin wrinkles to templating and material characterization. *Soft Matter* **2**, 310–323 (2006).
33. C. Hubbard, V. Naples, E. Ross, B. Carlon, Comparative analysis of paw pad structure in the clouded leopard (*Neofelis nebulosa*) and domestic cat (*Felis catus*). *Anat. Rec.* **292**, 1213–1228 (2009).
34. J. C. Quindlen, B. Güçlü, E. A. Schepis, V. H. Barocas, Computational parametric analysis of the mechanical response of structurally varying Pacinian corpuscles. *J. Biomech. Eng.* **139**, 071012 (2017).
35. H. Kwak, S. Shin, H. Lee, J. Hyun, Formation of a keratin layer with silk fibroin-polyethylene glycol composite hydrogel fabricated by digital light processing 3D printing. *J. Ind. Eng. Chem.* **72**, 232–240 (2019).
36. Y. Wang, K. L. Marshall, Y. Baba, G. J. Gerling, E. A. Lumpkin, Hyperelastic material properties of mouse skin under compression. *PLOS ONE* **8**, e67439 (2013).
37. N. Gjorevski, N. Sachs, A. Manfrin, S. Giger, M. E. Bragina, P. Ordóñez-Morán, H. Clevers, M. P. Lutolf, Designer matrices for intestinal stem cell and organoid culture. *Nature* **539**, 560–564 (2016).
38. G. Chen, S. Cui, L. You, Y. Li, Y.-H. Mei, X. Chen, Experimental study on multi-step creep properties of rat skins. *J. Mech. Behav. Biomed. Mater.* **46**, 49–58 (2015).
39. K. Hagisawa, A. Saito, M. Kinoshita, T. Fujie, N. Otani, S. Shono, Y.-K. Park, S. Takeoka, Effective control of massive venous bleeding by "multioverlapping therapy" using polysaccharide nanosheets in a rabbit inferior vena cava injury model. *J. Vasc. Surg. Venous Lymphat. Disord.* **1**, 289–297 (2013).
40. Y. Wang, G. A. Ameer, B. J. Sheppard, R. Langer, A tough biodegradable elastomer. *Nat. Biotechnol.* **20**, 602–606 (2002).
41. H. Smodlaka, W. A. Khamas, H. Jungers, R. Pan, M. Al-Tikriti, J. A. Borovac, L. Palmer, M. Bukac, A novel understanding of phocidae hearing adaptations through a study of northern elephant seal (*Mirounga angustirostris*) ear anatomy and histology. *Anat. Rec.* **302**, 1605–1614 (2019).
42. M. J. Levin, "Gross and microscopic observations on the lingual structure of the West Indian Manatee (*Trichechus manatus latirostris*)," thesis, Virginia Tech (2004).
43. J. Meixner, "Lame's wave functions of the ellipsoid of revolution" (1949).
44. J. Jachowicz, R. McMullen, D. Prettypaul, Indentometric analysis of in vivo skin and comparison with artificial skin models. *Skin Res. Technol.* **13**, 299–309 (2007).
45. J. Billingham, A. C. King, *Wave Motion* (Cambridge Univ. Press, 2000), no. 24.

Acknowledgments

Funding: This project has received funding from the European Union's Horizon 2020 research and innovation programme under grant agreement no. 801413; project "H-Reality," which has supported the contributions from J.W.A., M.J.A., and T.D.M.-J. **Author contributions:** J.W.A., M.J.A., and T.D.M.-J. conceptualized the research and wrote the manuscript. J.W.A. created the numerical codes and performed the data curation, formal analysis, the methodology, and the investigation. M.J.A. and T.D.M.-J. supervised the research. **Competing interests:** The authors declare that they have no competing interests. **Data and materials availability:** All data needed to evaluate the conclusions in the paper are present in the paper and/or the Supplementary Materials. Additional data related to this paper may be requested from the authors. The numerical code for repeating the analysis is publicly available at https://github.com/andrewsjw0568/Touch-is-skin-deep.git.

Submitted 11 March 2020
Accepted 26 August 2020
Published 9 October 2020
10.1126/sciadv.abb6912

Citation: J. W. Andrews, M. J. Adams, T. D. Montenegro-Johnson, A universal scaling law of mammalian touch. *Sci. Adv.* **6**, eabb6912 (2020).

Science Advances

A universal scaling law of mammalian touch

J. W. Andrews, M. J. Adams and T. D. Montenegro-Johnson

Sci Adv **6** (41), eabb6912.
DOI: 10.1126/sciadv.abb6912

Science Advances (ISSN 2375-2548) is published by the American Association for the Advancement of Science, 1200 New York Avenue NW, Washington, DC 20005. The title *Science Advances* is a registered trademark of AAAS.